Environmental Benign Synthesis of Lithium Silicates and Mg-Al Layered Double Hydroxide from Vermiculite Mineral for CO₂ Capture

Yu Zhang [1], Tuantuan Zhou [1], Benoit Louis [2], Feng Yu [3], Jianming Dan [3] and Qiang Wang [1,*]

[1] College of Environmental Science and Engineering, Beijing Forestry University, 35 Qinghua East Road, Haidian District, Beijing 100083, China; hjzhangyu@bjfu.edu.cn (Y.Z.); ztuant86@126.com (T.Z.)

[2] Laboratoire de Synthèse, Réactivité Organiques et Catalyse, Institut de Chimie, UMR 7177, Université de Strasbourg, 1 rue Blaise Pascal, 67000 Strasbourg, France; blouis@unistra.fr

[3] Key Laboratory for Green Processing of Chemical Engineering of Xinjiang Bingtuan, School of Chemistry and Chemical Engineering, Shihezi University, Shihezi 832003, China; yufeng05@mail.ipc.ac.cn (F.Y.); djm_tea@shzu.edu.cn (J.D.)

[*] Correspondence: qiang.wang.ox@gmail.com or qiangwang@bjfu.edu.cn; Tel.: +86-136-9913-0626

Abstract: This research introduces a completely new environmental benign synthesis route for obtaining two kinds of inter-mediate and high temperature CO_2 sorbents, Mg-Al layered double hydroxide (LDH) and Li_4SiO_4, from vermiculite. The mineral vermiculite was leached with acid, from which the obtained SiO_2 was used for the synthesis of Li_4SiO_4 and the leaching waste water was used for the synthesis of Mg-Al LDH. Therefore, no waste was produced during the whole process. Both Li_4SiO_4 and Mg-Al LDH sorbents were carefully characterized using XRD, SEM, and BET analyses. The CO_2 capturing performance of these two sorbents was comprehensively evaluated. The influence of the Li/Si ratio, calcination temperature, calcination time, and sorption temperature on the CO_2 sorption capacity of Li_4SiO_4, and the sorption temperature on the CO_2 sorption capacity of LDH, were investigated. The optimal leaching acid concentration for vermiculite and the CO_2 sorption/desorption cycling performance of both the Li_4SiO_4 and Mg-Al LDH sorbents were determined. In sum, this demonstrated a unique and environment-friendly scheme for obtaining two CO_2 sorbents from cheap raw materials, and this idea is applicable to the efficient utilization of other minerals.

Keywords: greenhouse gases; CO_2 sorbents; Li_4SiO_4; vermiculite mineral; cycling stability

1. Introduction

Carbon dioxide (CO_2) has been regarded as one of the most important greenhouse gases that contributes to the effects of global warming and climate change [1]. Fossil fuel power plants are responsible for >85% of the worldwide electrical energy demand [2]. Fossil fuel combustion is a major CO_2 source, which accounts for >40% of the total manmade CO_2 among all of the different types of CO_2 emissions [3]. In recent years, pre-combustion CO_2 capture from sorption enhanced hydrogen production (SEHP) processes has attracted considerable attention for capturing CO_2 from flue gas [4–11]. For the SEHP technique, one of the key challenges is the selection of a suitable solid CO_2 sorbent [12,13]. To date, several types of high-temperature CO_2 sorbents have been investigated, for instance, layered double hydroxide- (LDH) derived mixed oxides [14,15], and MgO [16] for the sorption enhanced water gas shift (SEWGS) process, and CaO [17,18], alkali zirconates [19], alkali dititanates [20], and alkali silicates [21,22] for the sorption enhanced steam reforming (SESR) process.

Compared with many other high-temperature CO_2 sorbents, Li_4SiO_4 is considered as one of the most promising sorbents due to its high sorption capacity, good thermal stability and reproducibility [1]. The Li_4SiO_4 sorbent mainly works in the temperature range of 500–750 °C for the SESR process. The CO_2 capture mechanism on Li_4SiO_4 can be explained by the reversible reaction between the Li_4SiO_4 crystal structure and CO_2, as described in reaction (1). The maximum CO_2 sorption capacity can thus be theoretically calculated as 36.7 wt %. However, the CO_2 capture capacities of synthesized Li_4SiO_4 reported in the literature are often much lower than the theoretical value, due to the mass transport limitation and severe sintering issues. In order to achieve an appreciable CO_2 capture performance of Li_4SiO_4 sorbents, several attempts have been made, including microstructural modification, alkali promotion, transition metal doping, and Li substitution by Na, etc. [12].

$$Li_4SiO_4 + CO_2 \leftrightarrow Li_2SiO_3 + Li_2CO_3 \tag{1}$$
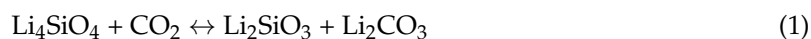
LDH-derived mixed oxides have been intensively studied as intermediate temperature CO_2 for the SEWGS process. According to mechanistic studies, the active Mg–O basic sites are believed to be responsible for CO_2 capture and the possible reaction can be described using Equation (2) [15,23]. Previously, great effort was devoted to the improvement of the CO_2 capture capacity and the long-term stability of LDH-based sorbents. For instance, the research activities mainly focused on the influence of cations (both divalent and trivalent), influence of anions (both organic and inorganic), influence of LDH morphology and particle size, the promoting effect of alkali carbonates, and the preparation of LDH-based inorganic hybrids [12,24,25].

$$Mg\text{-}O + CO_2 \text{ (g)} \rightarrow Mg\text{-}O \cdots\cdots CO_2 \text{ (sorbed)} \tag{2}$$
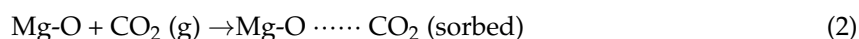
In addition to the work on improving the CO_2 capture capacity and stability, another research effort has been made to reduce the cost of sorbents by using cheap raw materials, for instance, industrial solid wastes or minerals. So far, there are a few reports on the synthesis of Li_4SiO_4 from waste silicon-containing materials including fly ash [26], rice husk ashes [27], and halloysite [28]. The Li_4SiO_4 which was synthesized with rice husk ashes achieved a 30.5 wt % maximum sorption at 680 °C and the Li_4SiO_4 which was synthesized with halloysite reached a maximum adsorption capacity of 34.75 wt % at 700 °C. However, there are almost no reports on the synthesis of LDH-derived CO_2 sorbents from either industrial solid wastes or minerals.

Vermiculite, a lamellar hydrated aluminum iron magnesium silicate, is a clay mineral with a 2:1 crystalline structure, which contains silicon dioxide (SiO_2), magnesium oxide (MgO), aluminum oxide (Al_2O_3), and some other metal oxides [29–31]. Vermiculite has an unusual property of expanding due to the interlamellar generation of steam. Due to the large content of the silicon element, vermiculite has been a cheap precursor for the synthesis of SiO_2 [24,32–34]. However, in order to remove the impure elements, a leaching pretreatment in strong acids is normally required. During this pretreatment process, a large amount of acidic wastewater with metal ions including Mg, Al, and Fe, is produced. The discharge of such wastewater causes severe environmental problems [27,35–37]. Thus, an environmentally benign scheme for the utilization of the vermiculite mineral is highly desired for a more sustainable society.

In this contribution, we developed a novel environmental benign synthesis route for obtaining two types of CO_2 capturing materials (lithium silicates and LDHs) from vermiculite. Throughout the whole synthesis process, no waste is emitted. The performance of the obtained lithium silicates and LDH-based CO_2 sorbents were evaluated under each of their suitable conditions. The long-term stability of the sorbents was investigated during the CO_2 sorption and desorption cycles.

2. Results and Discussion

2.1. Environmentally Benign Synthesis and Characterization of Li$_4$SiO$_4$ and LDHs

The environmentally benign synthesis scheme for obtaining Li$_4$SiO$_4$ and Mg-Al-CO$_3$ LDH from the vermiculite mineral is illustrated in Figure 1.The raw vermiculite mineral was first thermally pretreated at 900 °C to produce expanded vermiculite (EXVMT) with a higher specific surface area. The chemical composition of the samples was determined by X-ray fluorescence (XRF) spectroscopy (Panalytical Axios-mAX), which included SiO$_2$ (40.8 wt %), MgO (21.7 wt %), Al$_2$O$_3$ (20.8 wt %), K$_2$O (6.5 wt %), Fe$_2$O$_3$ (5.0 wt %), CaO (2.9 wt %), Na$_2$O (1.4 wt %), and TiO$_2$ (0.9 wt %). Then, the obtained EXVMT was leached in acidic solution at 80 °C, by which SiO$_2$ powder and an acidic wastewater containing Mg^{2+}, Al^{3+}, and other metals, were formed (Figure 1a). Following this, Li$_4$SiO$_4$ could be synthesized using a solid-state method by reacting the above obtained SiO$_2$ powder with lithium nitrate (Figure 1b), and Mg-Al-CO$_3$ LDH could be prepared using a co-precipitation method from the above obtained acidic wastewater (Figure 1c). During the whole synthesis procedure, both the obtained SiO$_2$ and the acidic wastewater were utilized, representing a promising and environmentally benign route for converting vermiculite minerals into high-value added products.
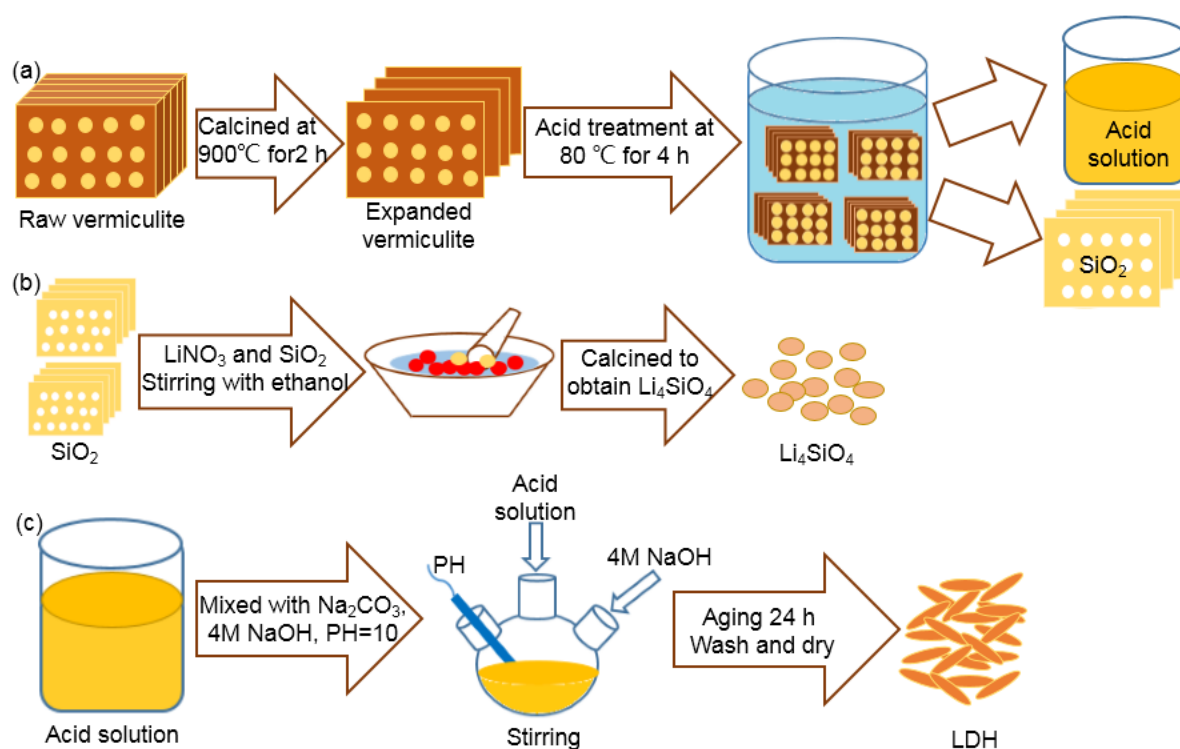

Figure 1. Schematic illustration of the synthesis of Li$_4$SiO$_4$ and LDH from vermiculite, (**a**) the vermiculite is treated with acid to obtain a silica and an acidic solution, (**b**) the synthesis of Li$_4$SiO$_4$ from the SiO$_2$ obtained in step (**a**), and (**c**) the synthesis of LDH from the acidic solution obtained in step (**a**).

In this synthesis process, one of the key parameters that affects the yield and quality of the SiO$_2$ and LDH products is the concentration used during leaching. In this work, four different concentrations of acid, including 1, 3, and 5 M HNO$_3$, and 6 M aqua regia, were used, and the obtained amounts of SiO$_2$ and LDH are summarized in Table 1. With the increase in the concentration of acid, the weight of the obtained SiO$_2$ decreased from 5.83 g with 1 M HNO$_3$, to 3.13 g with 6 M aqua regia. The XRD analyses of these SiO$_2$ samples suggest that a mild acid leaching treatment induces a low purity SiO$_2$. In contrast, a severe acidic treatment led to the leaching out of almost all of the elements,

thus producing a high-purity SiO_2. This is the reason why a smaller SiO_2 sample was obtained when the concentration of the acid was high. In contrast, the weight of the obtained LDHs increased with an increase in the concentration of the acid. This is because more elements were leached out into the acidic wastewater, which was consequently precipitated into LDHs by reacting with Na_2CO_3 and NaOH. This result clearly indicates that the concentration of leaching acid greatly influences the final products, which may eventually influence the CO_2 capture performance of the final Li_4SiO_4 and LDH-derived sorbents.

Table 1. The quantities of the obtained SiO_2 and Mg-Al-CO_3 LDH when the vermiculite was treated with different concentrations of leaching acids.

Acid	1 M (HNO_3)	3 M (HNO_3)	5 M (HNO_3)	6 M (Aqua Regia)
SiO_2 (g g^{-1})	0.583	0.511	0.419	0.373
LDH (g g^{-1})	0.365	0.422	0.475	0.667

The synthesis process was monitored using various material characterization tools. Figure 2a shows the XRD patterns of VMT and EX-VMT. VMT is a clay mineral consisting of negatively charged silicate layers, with a thickness of about 1 nm. The negative charge arises from the substitution of Al^{3+} by Si^{4+} in tetrahedral sites. Before thermal treatment, the raw VMT showed an interlayer spacing of 1.10 nm, and the characteristic d_{002} reflection peak was observed at 8.02°. This interlayer spacing is slightly narrower than the reported value of 1.44 nm. This phenomenon might be due to the drying in an oven at 100 °C prior to XRD analysis, which caused the partial dehydration of the sample. After thermal treatment at 900 °C, the interlayer distance of the EX-VMT was further narrowed. The characteristic d_{002} peak shifted to a higher 2θ degree of 8.78°, corresponding to an interlayer spacing of 1.01 nm. This change can be attributed to the loss of the hydration water of the interlayer cations [38,39]. Figure 2b shows the SEM image of raw VMT, from which the layered structure can be clearly observed, in which all of the layers are tightly packed. However, an abrupt heating of vermiculite at 900 °C induced the exfoliation of VMT, as shown in Figure 2c. In addition, the deformation of the surface of EX-VMT can also be seen, which was due to the spontaneous release of interlayer water molecules [40]. The XRD pattern of residual solids confirmed that its majority phase was amorphous SiO_2 (Figure 2d).

Then, the obtained Li_4SiO_4 and LDH were also characterized by XRD, BET, and SEM techniques, as shown in Figure 3. The XRD patterns in Figure 3a) clearly indicate that both Li_4SiO_4 and LDH were successfully synthesized. For Li_4SiO_4, characteristic peaks at 22.18°, 33.79°, and 38.19°, were observed, which can be attributed to the reflections of −110, 200, and −121 planes. For LDH, the characteristic peaks at 11.68°, 23.53°, 35.61°, 39.62°, and 47.19° were observed, being attributed to the reflections of 003, 006, 009, 015, and 018 planes. The interlayered distance d_{003} is 0.74 nm, which is similar to the literature reports [41]. Figure 3b shows the N_2 adsorption/desorption isothermal of synthesized Li_4SiO_4, which suggests that the sample is non porous and that its specific surface area was quite low (1.3 m$^2 \cdot$g^{-1}). The morphologies of the Li_4SiO_4 and LDH samples were studied using SEM analysis, as shown in Figure 3c,d. Li_4SiO_4 exhibited relatively dense polyhedral particles, which is common for samples synthesized by the solid-state method. The SEM analysis is consistent with the BET result. The Mg-Al-CO_3 LDH showed a petaloid structure consisting of a nanosheet [15,42–44]. The formation of this petaloid-like morphology can be attributed to the synthesis pH of 10. When the pH value equals the isoelectric point of Mg-Al-CO_3 LDH, its surface will be close to neutral and the LDH particles will preferably grow into a petaloid structure [45]. All of the aforementioned analyses indicate that both Li_4SiO_4 and Mg-Al-CO_3 LDH can be successfully synthesized from the vermiculite mineral. In the following section, their CO_2 capturing performance will be comprehensively evaluated under various conditions.
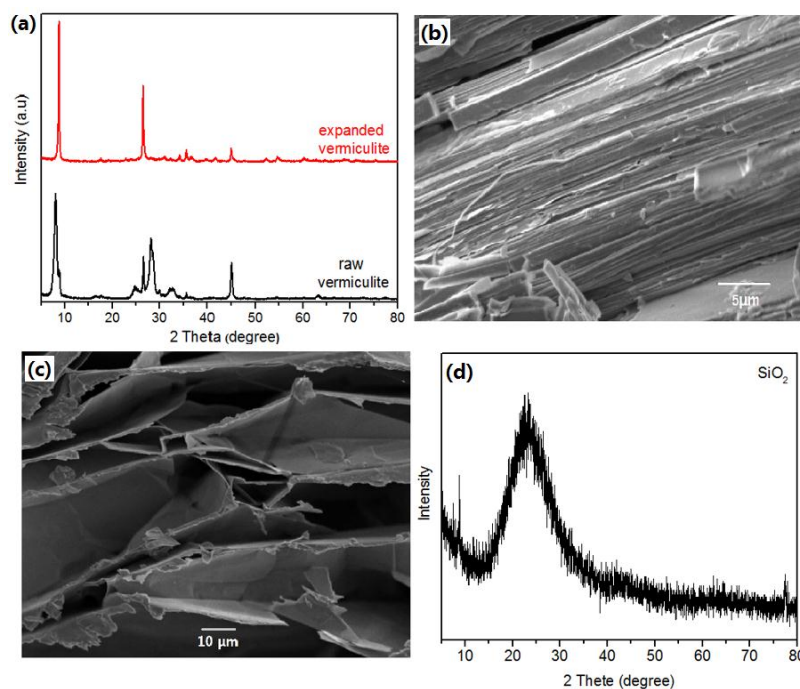
Figure 2. (**a**) The XRD patterns of VMT and EX-VMT, (**b**) SEM image of VMT, (**c**) SEM image of EX-VMT, and (**d**) XRD pattern of SiO_2 sample obtained with 6 M aqua regia.
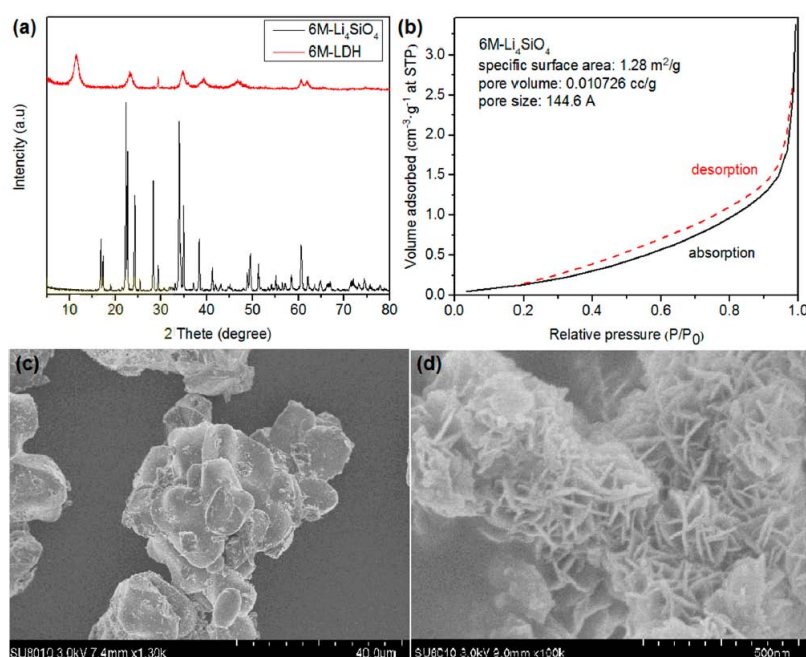

Figure 3. XRD, BET, and SEM analysis of synthesized Li_4SiO_4 and $Mg-Al-CO_3$ LDH when 6 M aqua regia was used as the leaching acid, (**a**) XRD patterns of synthesized Li_4SiO_4 and $Mg-Al-CO_3$ LDH, (**b**) BET analysis of synthesized Li_4SiO_4, (**c**) SEM image of the Li_4SiO_4 sample, and (**d**) SEM image of the LDH sample.

2.2. CO₂ Capture Performance of Synthesized Li₄SiO₄ and LDH-Based Sorbents

In order to investigate the effect of the Li/Si molar ratio on the CO_2 sorption performance, Li_4SiO_4-based sorbents were synthesized with different Li/Si mole ratios, ranging from three to 10.

The SiO_2 was obtained from EX-VMT, which was treated with 6 M aqua regia. All Li_4SiO_4-(EX-VMT)-*x* (*x* = 3, 4, 5, 6, 7, 8, 9, and 10) were synthesized by a thermal treatment of 750 °C for 6 h. The CO_2 sorption capacities of all samples were evaluated at 650 °C for 2 h, under pure CO_2. Figure 4a and Table 2 show that when the Li/Si molar ratio was three, the sorption capacity was relatively low (ca. 25.21 wt %). When the Li/Si molar ratio was increased to four, the CO_2 sorption capacity rapidly improved to 30.47 wt %, reaching 93.7% of the theoretical sorption capacity of Li_4SiO_4 (32.52 wt %). However, when the Li/Si molar ratio was in the range of five to nine, the CO_2 sorption capacities did not show any significant increase, and were all around 25.97–36.21 wt %. Some of the values were even higher than the theoretical sorption capacity of Li_4SiO_4 (32.52 wt %), which is probably due to the formation of Li_8SiO_6. The following XRD analysis of all of the samples clearly confirms this hypothesis. In particular, when the Li/Si molar ratio was 10, the CO_2 sorption capacity sharply improved to 57.93 wt %. However, although the formation of Li_8SiO_6 can significantly improve the CO_2 sorption capacity, its sorption/desorption cycling performance was normally very poor. In other words, due to the even worse reversible CO_2 sorption capacity, the formation of Li_8SiO_6 is normally prevented and Li_4SiO_4 is preferred.
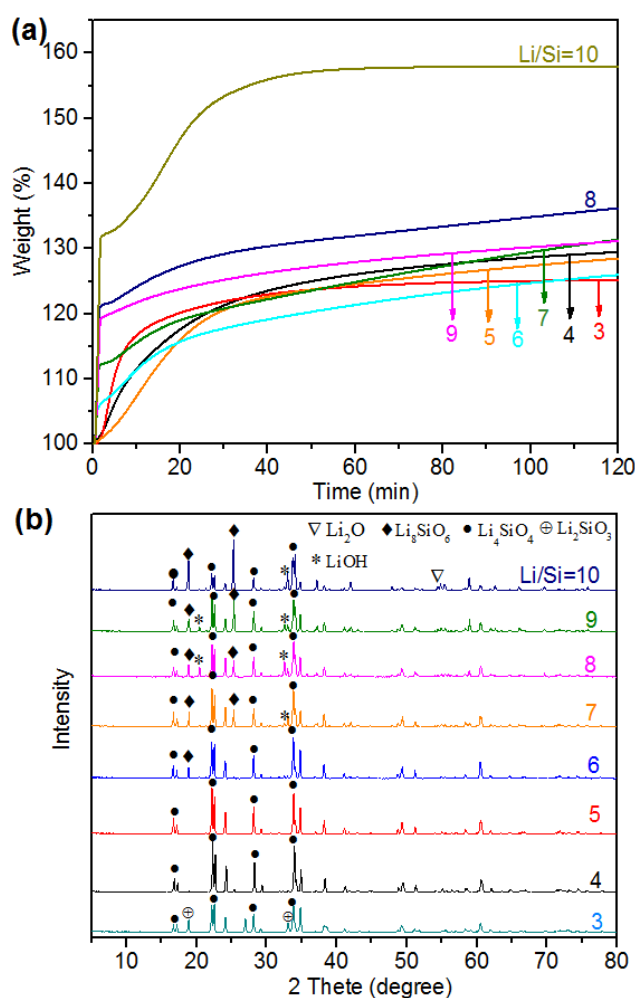

Figure 4. (**a**) CO_2 sorption capacity of Li_4SiO_4-(EX-VMT)-*x* (*x* = 3, 4, 5, 6, 7, 8, 9, and 10) samples at 650 °C, (**b**) XRD patterns of Li_4SiO_4-(EX-VMT)-*x* (*x* = 3, 4, 5, 6, 7, 8, 9, and 10) samples.

Table 2. CO_2 sorption capacity of Li_4SiO_4-(EX-VMT)-*x* (*x* = 3, 4, 5, 6, 7, 8, 9, and 10) samples at 650 °C.

Li/Si Molar Ration	3:1	4:1	5:1	6:1	7:1	8:1	9:1	10:1
CO_2 sorption capacity (wt %)	25.21	30.47	28.56	25.97	31.43	36.21	31.56	57.93

In order to explain the influence of the Li/Si molar ratio on the CO_2 sorption capacity of synthesized Li_4SiO_4-based sorbents, an XRD analysis of all samples was performed, as shown in Figure 4b. For all samples, the characteristic peaks of Li_4SiO_4 were detected, suggesting the existence of the Li_4SiO_4 phase. When the Li/Si molar ratio was three, a small portion of Li_2SiO_3 was detected. Li_2SiO_3 has no CO_2 sorption ability at high temperatures, which explains the relatively low CO_2 sorption capacity of Li_4SiO_4-(EX-VMT)-3 [46]. When the Li/Si molar ratio reached four and five, relatively pure Li_4SiO_4 was synthesized. Moreover, when the Li/Si molar ratio increased from six to nine, the phases of both LiOH and Li_8SiO_6 appeared. In particular, at Li/Si = 10, the characteristic peaks of Li_2O and Li_8SiO_6 became more obvious, thus explaining the high CO_2 sorption capacity of Li_4SiO_4-(EX-VMT)-10. According to the literature, the regeneration performance of Li_2O and Li_8SiO_6 is very poor, which means that the sample is not promising for practical applications [46]. In order to obtain the Li_4SiO_4-based CO_2 sorbent that has a high CO_2 sorption capacity and good cycling performance, the Li_4SiO_4-(EX-VMT)-4 sample was selected as the optimal sample for further study.

Then, the synthesis temperature for the Li_4SiO_4-based sorbents was optimized to further improve the CO_2 sorption capacity. Different Li_4SiO_4-(EX-VMT)-4 samples were synthesized at temperatures of 650, 700, 750, and 800 °C. Their CO_2 sorption capacities were evaluated using TGA analysis at 650 °C, as shown in Figure 5a. The CO_2 sorption capacity initially increased slightly from 34.12 wt % to 34.39 wt %, with an increase in the synthesis temperature from 650 to 700 °C. However, the CO_2 sorption capacity started to decrease with a further increase in the synthesis temperature. At 750 and 800 °C, the CO_2 sorption capacity diminished to 29.46 wt % and 18.74 wt %, respectively. These results confirm that the best synthesis temperature of the Li_4SiO_4-(EX-VMT)-4 sorbent is 700 °C. Figure 5b shows the XRD patterns of the sorbents synthesized at different temperatures. For all samples, the Li_4SiO_4 phase is the main phase. With an increase in the synthesis temperature, the peak intensity became slightly sharper, suggesting that the decrease in the CO_2 sorption capacity might be due to the sintering of sorbents at high temperatures.

Besides, the influence of the calcination time on the CO_2 sorption capacity of Li_4SiO_4-(EX-VMT)-4 sorbents was also studied, as shown in Figure 5c. When the samples were synthesized for 5, 6, and 7 h, the CO_2 sorption capacity of all samples was quite similar, exhibiting values of 33.63 wt %, 34.39 wt %, and 33.95 wt %, respectively. The XRD patterns of these three samples are presented in Figure 5d. The results confirmed that an optimized synthesis temperature of 700 °C led to the Li_4SiO_4 main phase being barely affected by the calcination time.

For a practical application purpose, the CO_2 sorption capacity of the Li_4SiO_4-(EX-VMT)-4 sorbent under different operating conditions was investigated. Figure 6a shows the influence of sorption temperature on the CO_2 sorption capacity of the Li_4SiO_4-(EX-VMT)-4 sorbent. The sorbent showed the best sorption performance and the fastest sorption kinetics at 650 °C, with a CO_2 sorption capacity of 34.39 wt %. Compared with other Li_4SiO_4-based sorbents that were also synthesized from cheap SiO_2 precursors, the Li_4SiO_4-(EX-VMT)-4 sample obtained in this research exhibited a higher CO_2 capacity [27,28]. When the sorption temperature dropped to 600 °C, the CO_2 sorption capacity of Li_4SiO_4-(EX-VMT)-4 was only 22.11 wt %, which may be due to the kinetic limitation at a low sorption temperature. However, when the sorption temperature reached 700 °C, the Li_4SiO_4-(EX-VMT)-4 sorbent displayed almost no sorption capacity (2.51 wt %). This may be due to the activation of CO_2 desorption from Li_4SiO_4 at 700 °C. Considering these findings, it can be concluded that the best sorption temperature for the Li_4SiO_4-(EX-VMT)-4 sorbent is 650 °C.
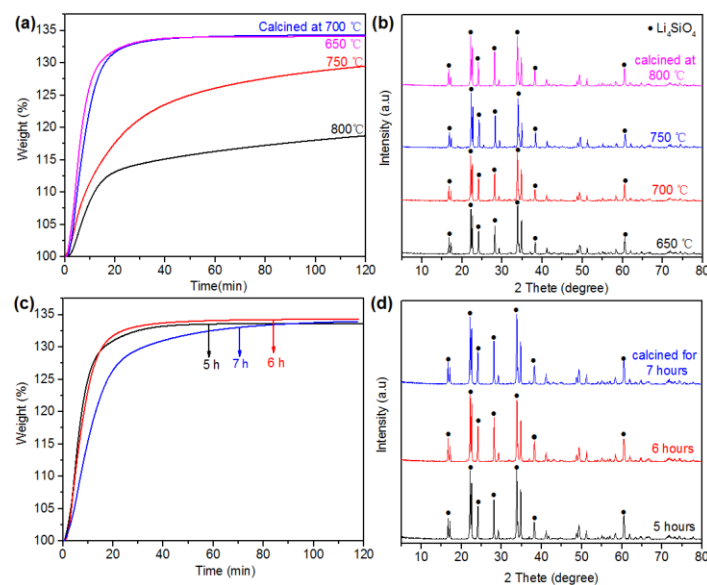
Figure 5. (**a**) The CO_2 sorption performance of Li_4SiO_4-(EX-VMT)-4 samples synthesized at different temperatures (CO_2 sorption was evaluated at 650 °C), (**b**) XRD patterns of Li_4SiO_4-(EX-VMT)-4 samples synthesized at different temperatures, (**c**) The CO_2 sorption performance of Li_4SiO_4-(EX-VMT)-4 samples synthesized at 700 °C for different times (CO_2 sorption was evaluated at 650 °C), and (**d**) XRD patterns of Li_4SiO_4-(EX-VMT)-4 samples synthesized at 700 °C for different times.
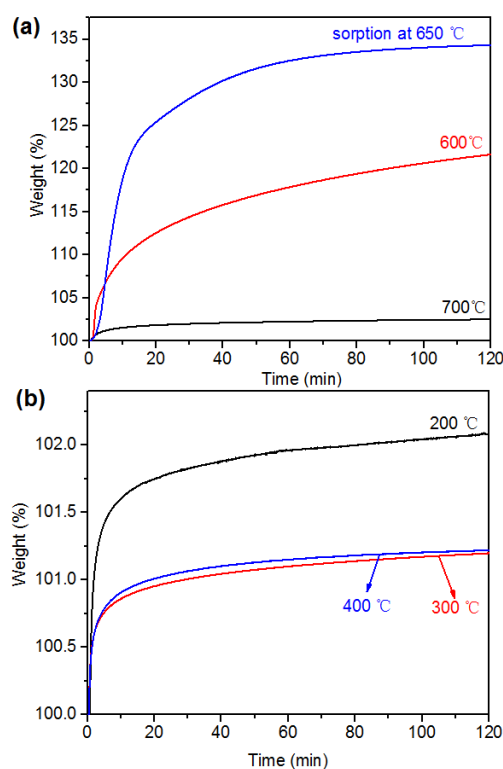

Figure 6. (**a**) CO_2 sorption performance of Li_4SiO_4-(EX-VMT)-4 sorbent evaluated at different sorption temperatures of 600, 650, and 700 °C, and (**b**) the influence of sorption temperature on the CO_2 capture performance of Mg-Al-CO_3 LDH synthesized from the vermiculite leaching wastewater.

In addition to the Li_4SiO_4-based sorbent, the CO_2 capture performance of the Mg-Al-CO_3 LDH-derived sorbents was also studied in this work, as shown in Figure 6b. All of the samples were calcined at 400 °C before the CO_2 sorption tests were performed, and the performances at different temperatures of 200, 300, and 400 °C were evaluated. The results indicated that the Mg-Al-CO_3 LDH-derived CO_2 sorbent led to the highest CO_2 sorption capacity at 200 °C, being 2.08 wt %. This value is similar to the LDH-derived CO_2 sorbent reported in the literature [45]. However, the CO_2 sorption capacity became much lower when the sorption temperature was higher, with values of 1.21 wt % and 1.23 wt % at 300 and 400 °C, respectively. This result suggests that the LDHs synthesized from the vermiculite leaching wastewater can deliver a similar CO_2 capture performance to those of pure LDH samples.

2.3. Optimization of the Synthesis Strategy

As we have shown in the above section that the concentration of leaching acid has an important influence on the chemical composition of obtained SiO_2 and LDHs samples, we found it worthy to investigate the influence of the leaching acid on the CO_2 capture performance of synthesized Li_4SiO_4 and LDH-based sorbents. From an economical and environmental point of view, using a lower concentration of leaching acid, while maintaining a relatively good CO_2 capture performance, is warranted. Therefore, in this section, the synthesis strategy for obtaining two types of CO_2 sorbents, Li_4SiO_4 and LDH, from a vermiculite mineral was further optimized by using different concentrations of leaching acids, such as 1, 3, and 5 M HNO_3 and 6 M aqua regia. The obtained samples were denoted as Li_4SiO_4-(EX-VMT)-4 (*x*M) (*x* = 1, 3, 5, and 6) and Mg-Al-CO_3 LDH-*x*M (*x* = 1, 3, 5, and 6), respectively.

Figure 7a shows the CO_2 capture performance of Li_4SiO_4-(EX-VMT)-4 (*x*M) (*x* = 1, 3, 5, and 6) samples in pure CO_2 at 650 °C. When comparing all of the samples, the CO_2 sorption capacity of Li_4SiO_4-(EX-VMT)-4 (3M) has the lowest sorption capacity (31.87 wt %). With an increase in the concentration of acid, the CO_2 sorption capacity of Li_4SiO_4-(EX-VMT)-4 (5M) and Li_4SiO_4-(EX-VMT)-4 (6M) also increased, reaching 34.21 wt % and 34.39 wt %, respectively. It is surprising that the highest CO_2 sorption capacity was achieved with the 1 M acid. This is due to the synthesis scheme we used for the synthesis of the Li_4SiO_4-(EX-VMT)-4 (*x*M) samples. When calculating the Li/Si ratio of four, we assumed that all of the obtained solid product was SiO_2. However, the SiO_2 sample obtained with 1 M acid still contained impurities, which led to a Li/Si ratio higher than four. The high CO_2 sorption capacity of the Li_4SiO_4-(EX-VMT)-4 (1M) sample may be due to the existence of the Li_2O phase.

In order to gain a deeper understanding of the influence of the concentration of acid on the CO_2 sorption performance, the XRD patterns of Li_4SiO_4-(EX-VMT)-4 (*x*M) samples were examined, as shown in Figure 7b. When the concentration of acid was 6 M, the sample only consisted of Li_4SiO_4. When decreasing the concentration of acid from 5 to 1 M, the MgO phase appeared, which proved that a low acidic concentration will produce impurities in SiO_2. Hence, this consequently influences the CO_2 sorption capacity of the samples. However, when the concentration of acid was too low, the content of SiO_2 became lower, which means that the Li/Si molar ratio was increased. Excess lithium led to the formation of the Li_2O phase in the Li_4SiO_4-based sorbent. Previous studies have confirmed that Li_2O has a higher CO_2 sorption capacity, but worse regeneration property, than Li_4SiO_4.

Figure 8a shows the CO_2 sorption capacities of Mg-Al-CO_3 LDH-*x*M (*x* = 1, 3, 5, and 6) samples. It appears that the CO_2 sorption capacity gradually increased with an increase in the concentration of acid from 1 to 6 M. For example, with a concentration of acid of 1, 3, 5, and 6 M, the CO_2 sorption capacity was 1.3wt %, 1.57 wt %, 1.63 wt %, and 2.08 wt %, respectively. Mg-Al-CO_3 LDH-6 M showed the highest CO_2 sorption capacity of 2.08 wt % at 200 °C. Figure 8b shows the XRD patterns of Mg-Al-CO_3 LDH-*x*M (*x* = 1, 3, 5, and 6). All of the synthesized samples formed a typical layered double hydroxide structure. This data suggests that there is no significant difference in their phase structure. The difference in their CO_2 capture capacity might be due to the Mg content. As is shown in Figure 7b, when the concentration of acid was low, the Mg element could not be completely leached

out from the SiO_2. Thus, the relatively lower Mg content in Mg-Al-CO_3 LDH-*x*M results in a lower CO_2 sorption capacity.
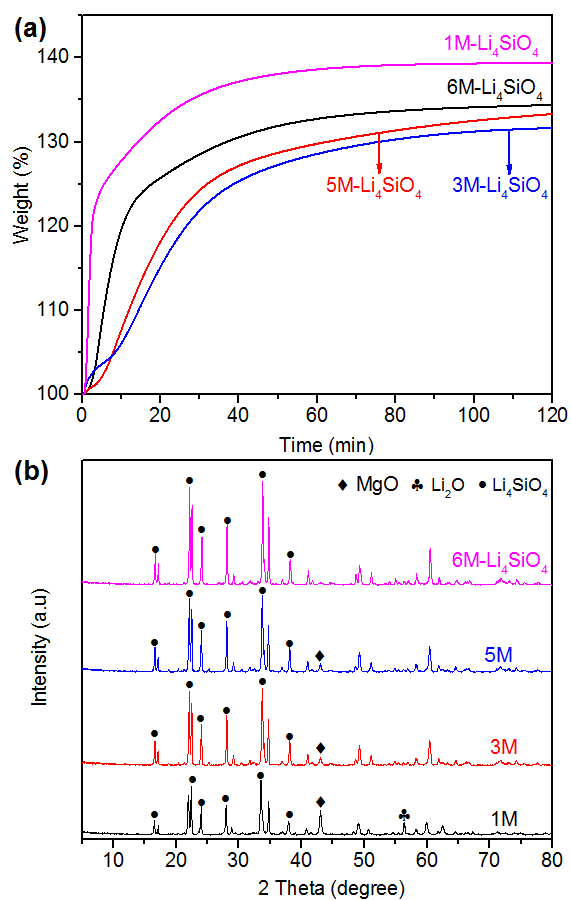

Figure 7. (**a**) The influence of leaching acid concentration on the CO_2 sorption capacity of Li_4SiO_4-(EX-VMT)-4 (*x*M) samples, and (**b**) the XRD patterns of Li_4SiO_4-(EX-VMT)-4 (*x*M) samples.

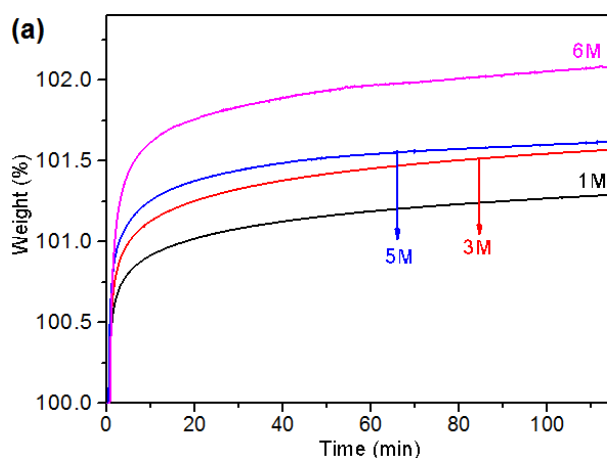**Figure 8.** *Cont.*

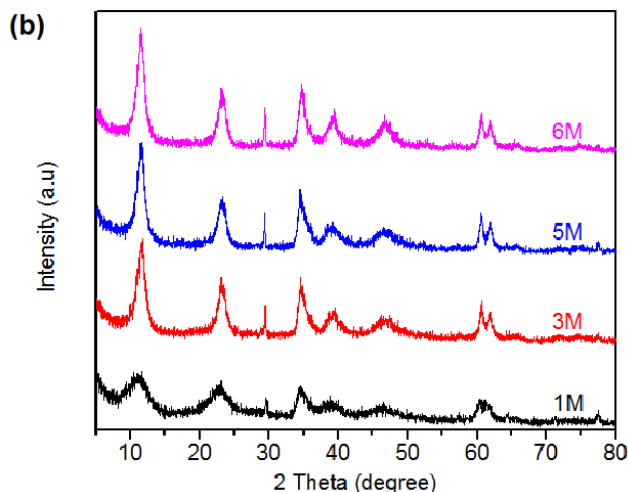**Figure 8.** (**a**) The influence of leaching acid concentration on the CO_2 sorption capacity of Mg-Al-CO_3 LDH-*x*M (*x* = 1, 3, 5, and 6) samples, and (**b**) the XRD patterns of Mg-Al-CO_3 LDH-*x*M (*x* = 1, 3, 5, and 6) samples.

2.4. Cycling Stability of Obtained CO_2 Sorbents

For the practical application of CO_2 sorbents, particularly at high temperatures, the CO_2 sorption/desorption cycling stability is another important aspect. Thus, the cycling stability of the Li_4SiO_4-(EX-VMT)-4 (*x*M) (*x* = 1, 3, and 6) samples was investigated. Both sorption and desorption were performed at 650 °C for 30 min. Figure 9a shows that when the concentration of acid was 6 M, the cycle stability of the obtained Li_4SiO_4-(EX-VMT)-4 (6M) was poor. The CO_2 sorption capacity started to decline quickly after its seventh cycle, which might be due to the sintering of the sorbent. After 10 cycles, the capacity decreased from its initial 29.37 wt %, to 25.86 wt %. However, with the decrease in leaching acid concentration, the cycling stability of the sorbents was slightly improved. For instance, the decline rate of Li_4SiO_4-(EX-VMT)-4 (3M) was slower than that of Li_4SiO_4-(EX-VMT)-4 (6M), and its CO_2 sorption capacity started to decline during its tenth cycle. This improved stability might be attributed to the separating and supporting effect from the impurity phases within this sample. This speculation was further confirmed by the result from Li_4SiO_4-(EX-VMT)-4 (1M). When the leaching acid concentration was as low as 1 M, more impurities remained in the sorbent, thus leading to a decreased CO_2 sorption capacity (1.17 wt %). However, it is very clear that the overall stability was improved, without almost any change during the 15 cycles. Thus, these data suggested a promising way to design highly stable Li_4SiO_4-based CO_2 sorbents, by introducing certain inert separating and supporting materials.

In addition, the cycling stability of the synthesized LDH-derived CO_2 sorbent was also studied, and Mg-Al-CO_3 LDH-6M was taken as the representative. The sorption was performed at 200 °C in pure CO_2 flow, and the desorption was performed at 400 °C in pure N_2, both of which were performed for 30 min. Figure 9b shows that the Mg-Al-CO_3 LDH-6M-derived sorbent has an excellent cycling stability during the fifteenth cycle. Almost no change was observed and the CO_2 sorption capacity remained at 1.26 wt %. To summarize, we can conclude that via the newly developed environmentally benign synthesis strategy, two types of high-temperature CO_2 sorbents, Li_4SiO_4 and LDH, can be obtained from the cheap raw material vermiculite, and their performance can be tuned by optimizing the synthesis procedure and parameters.
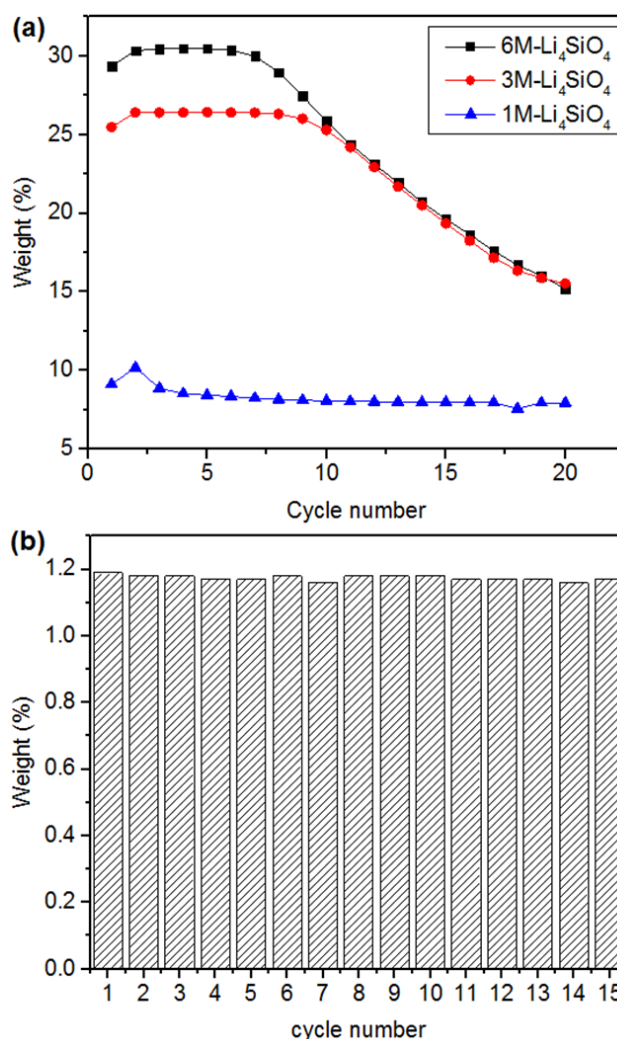
Figure 9. (**a**) CO_2 sorption/desorption cycling performance of Li_4SiO_4-(EX-VMT)-4 (*x*M) (*x* = 1, 3, and 6) samples, and (**b**) CO_2 sorption/desorption cycling performance of the Mg-Al-CO_3 LDH-6M sample.

3. Materials and Methods

3.1. Synthesis of Li_4SiO_4 and LDH from Vermiculite

Vermiculite (VMT) was taken from the Xinjiang Province, China. First, the vermiculite was calcined at 900 °C for 2 h to form expanded vermiculite (EXVMT), which has a higher specific surface area compared to vermiculite. The chemical composition of EXVMT was determined by X-ray fluorescence (XRF) spectroscopy (Panalytical Axios-mAX). Then, the obtained EXVMT (10 g) was leaching pretreated in 200 mL of acidic solution at 80 °C for 24 h. The acidic solution used for this pretreatment of vermiculite was selected from 6 M aqua regia solution, 5 M HNO_3, 3 M HNO_3, or 1 M HNO_3. When the leaching pretreatment process was ended, the suspension was filtered to separate the solid sample and the acidic washing wastewater. The obtained solid powder, which mainly contained SiO_2, was washed with distilled water until the filter liquor was neutral, and dried in an oven.

Li_4SiO_4 was synthesized using a solid-state method by reacting the above obtained SiO_2 powder with lithium nitrate ($LiNO_3$, AR). The chemical reaction of this process was described in reaction (3). The influence of the Li/Si molar ratio (Li/Si = 3, 4, 5, 6, 7, 8, 9, and 10), calcination temperature (650, 700, 750, and 800 °C), and calcination time (5, 6, and 7 h) on the formation of lithium silicates was systematically studied.

$$SiO_2 + 4LiNO_3 \rightarrow Li_4SiO_4 + 4NO_2 + O_2 \tag{3}$$
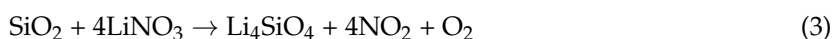
The Mg-Al-CO$_3$ LDHs were synthesized using a co-precipitation method from the above obtained acidic washing wastewater. First, the collected acidic washing wastewater was neutralized using 4 M NaOH until pH = 10. Then, 200 mL of this neutralized solution containing mainly Mg^{2+} and Al^{3+} was added drop-wise to 100 mL of 0.4 M Na$_2$CO$_3$ solution. The pH value was kept at a constant value of 10 during the whole process, by adding 4 M NaOH. The suspension was stirred for 24 h at room temperature for aging. The samples were washed with deionized water until the filter liquor was neutral. The sample was further dispersed in acetone, stirred for 2 h, and then thoroughly washed with acetone. Finally, the obtained LDH was dried at 100 °C in an oven. The corresponding LDO can be obtained by calcining at 400 °C for 5 h.

3.2. Characterization of Samples

The phase structure of the samples was analyzed by powder X-ray diffraction (XRD) measurements performed on a Shimadzu XRD-7000 instrument in reflection mode with Cu K radiation. The accelerating voltage was set at 40 kV with a 30 mA current (λ = 1.542 Å) from 1 to 70°, with a scan rate of 2° min^{-1} and a step size of 0.02°. The morphology of the samples was studied using scanning electron microscopy (SEM, Hitachi S-3400N II). Before observation, the dried samples were sputtered and coated with gold for ~30 s, under an argon atmosphere. The specific surface area and pore information of the samples were determined by N$_2$ sorption/desorption measurements (BET SSA-7000).

3.3. Evaluation of CO$_2$ Capture Performance

The CO$_2$ sorption capacity and the long-term cycling stability of the synthesized sorbents were evaluated using TGA apparatus (Q50 TA Instrument). For the Li$_4$SiO$_4$-based sorbent, after placing the sample in the sample pan of TAG, it was heat-treated from room temperature to 650 °C, and kept at this temperature for 30 min N$_2$. The CO$_2$ capture capacity of Li$_4$SiO$_4$ was then determined isothermally under pure CO$_2$ (40 mL/min) at 650 °C, for 120 min. For the LDH-derived sorbent, the sample was first calcined at 400 °C for 5 h to obtain LDO. The LDO sample was further calcined in situ at 400 °C for 1 h under a flow of high purity N$_2$ (40 mL min^{-1}), before performing the CO$_2$ sorption test. The temperature was then lowered to 200 °C, and the gas was switched from N$_2$ to CO$_2$ (40 mL min^{-1}), and the CO$_2$ sorption was measured for 2 h.

The cycling performance of Li$_4$SiO$_4$-based CO$_2$ sorbents was measured using a pressure swing adsorption process. CO$_2$ sorption was performed at 650 °C in CO$_2$ flow (40 mL/min) for 30 min and desorption was performed at the same temperature in N$_2$ (29 mL/min) for 30 min. For the LDH-derived sorbents, a temperature swing adsorption process was applied, with a sorption temperature of 200 °C and a desorption temperature of 400 °C. In a typical run, the sorbent was heated to 200 °C at a rate of 10 °C min^{-1} under N$_2$ and maintained for 60 min. When the temperature was reached and stabilized, the N$_2$ was switched to CO$_2$. After sorption for 30 min, the gas was switched to N$_2$, and the TGA analyzer was heated to 400 °C at a rate of 10 °C min^{-1} and kept at 400 °C for 30 min. After the completion of desorption, the temperature was decreased to 200 °C for the next cycle of CO$_2$ sorption.

4. Conclusions

In this contribution, we demonstrated that two kinds of high-temperature CO$_2$ sorbents (Li$_4$SiO$_4$-based and Mg-Al-CO$_3$ LDH-derived) can be economically and environmentally synthesized from a cheap mineral vermiculite. The Li/Si molar ratio, calcination temperature and time, and sorption temperature, have shown an important impact on the CO$_2$ sorption capacity of Li$_4$SiO$_4$-based and Mg-Al-CO$_3$ LDH-derived sorbents. When the Li/Si molar ratio reached four and five, relatively pure Li$_4$SiO$_4$ was synthesized. However, when the Li/Si molar ratio was high (six-nine), LiOH and Li$_8$SiO$_6$ phases appeared and their cycling performance became worse due to their poor regeneration property. The best calcination temperature was determined to be 750 °C. The optimized Li$_4$SiO$_4$ and Mg-Al-CO$_3$ LDH achieved a good CO$_2$ sorption capacity of 34.39 wt % at 650 °C and 2.08 wt % at 200 °C,

respectively. We also proved that the concentration of leaching acid greatly influenced the chemical composition of these two sorbents, which consequently affected their CO_2 sorption/desorption cycling performance. For the Li_4SiO_4-based sorbent, it exhibited a good initial CO_2 sorption capacity but poor cycling performance with a high leaching acid concentration and poor initial CO_2 sorption capacity, but a good cycling performance with a low leaching acid concentration. The improved cycling performance can be attributed to the remaining impurity phases in the Li_4SiO_4-based sorbent that work as inert separating and supporting materials. The cycling performance of the LDH-derived sorbent was very stable during (at least) 15 cycles.

Author Contributions: Q.W. conceived and designed the experiments; Y.Z. performed the experiments and wrote the paper; T.Z. and B.L. helped in analyzing the data; F.Y. and J.D. contributed to the synthesis and characterization of materials.

Conflicts of Interest: The authors declare no conflict of interest.

References

1. Kato, M.; Yoshikawa, S.; Nnkagawa, K. Carbon dioxide absorption by lithium orthosilicate in a wide range of temperature and carbon dioxide concentrations. *J. Mater. Sci. Lett.* **2002**, *21*, 485–487. [CrossRef]
2. Basinas, P.; Wu, Y.H.; Grammelis, P.; Anthony, E.J.; Grace, J.R.; Lim, C.J. Effect of pressure and gas concentration on CO_2 and SO_2 capture performance of limestones. *Fuel* **2014**, *122*, 236–246. [CrossRef]
3. Yang, H.; Xu, Z.; Fan, M.; Gupta, R.; Slimane, R.B.; Bland, A.E.; Wright, I. Progress in carbon dioxide separation and capture: A review. *J. Environ. Sci.* **2008**, *20*, 14–27. [CrossRef]
4. Zhang, S.; Zhang, Q.; Shen, C.; Ni, Y.H.; Wu, Y.Q.; Wu, Q.F.; Zhu, Z.B. Self-Activation Mechanism Investigations on Large K_2CO_3-Doped Li_4SiO_4 Sorbent Particles. *Ind. Eng. Chem. Res.* **2015**, *54*, 7292–7300. [CrossRef]
5. Rusten, H.K.; Ochoa-Fernandez, E.; Lindborg, H.; Chen, D.; Jakobsen, H.A. Hydrogen production by sorption-enhanced steam methane reforming using lithium oxides as CO_2-acceptor. *Ind. Eng. Chem. Res.* **2007**, *46*, 8729–8737. [CrossRef]
6. Kato, M.; Maezawa, Y.; Takeda, S.; Hagiwara, Y.; Kogo, R. Precombustion CO_2 capture using ceramic absorbent and methane steam reforming. *J. Ceram. Soc. Jpn.* **2005**, *113*, 252–254. [CrossRef]
7. Barelli, L.; Bidini, G.; Gallorini, F.; Servili, S. Hydrogen production through sorption-enhanced steam methane reforming and membrane technology: A review. *Energy* **2008**, *33*, 554–570. [CrossRef]
8. Bretado, M.E.; Vigil, M.D.D.; Martinez, V.H.C.; Ortiz, A.L. Thermodynamic analysis for the production of hydrogen through Sorption Enhanced Water Gas Shift (SEWGS). *Int. J. Chem. React. Eng.* **2008**, *6*, 77–90.
9. Chen, Y.; Zhao, Y.; Zhang, J.; Zheng, C. Hydrogen production through CO_2 sorption-enhanced methane steam reforming: Comparison between different adsorbents. *Sci. China Technol. Sci.* **2011**, *54*, 2999–3008. [CrossRef]
10. Kim, K.; Kim, D.; Park, Y.K.; Lee, K.S. A solid sorbent-based multi-stage fluidized bed process with inter-stage heat integration as an energy efficient carbon capture process. *Int. J. Greenh. Gas Control* **2014**, *26*, 135–146. [CrossRef]
11. Zhang, Q.; Shen, C.; Zhang, S.; Wu, Y.Q. Steam methane reforming reaction enhanced by a novel K_2CO_3-Doped Li_4SiO_4 sorbent: Investigations on the sorbent and catalyst coupling behaviors and sorbent regeneration strategy. *Int. J. Hydrog. Energy* **2016**, *41*, 4831–4842. [CrossRef]
12. Wang, J.Y.; Huang, L.; Yang, R.Y.; Zhang, Z.; Wu, J.W.; Gao, Y.S.; Wang, Q.; O'Hare, D.; Zhong, Z.Y. Recent advances in solid sorbents for CO_2 capture and new development trends. *Energy. Environ. Sci.* **2014**, *7*, 3478–3518. [CrossRef]
13. Wang, Q.; Tay, H.H.; Zhong, Z.Y.; Luo, J.Z.; Borgna, A. Synthesis of high-temperature CO_2 adsorbents from organo-layered double hydroxides with markedly improved CO_2 capture capacity. *Energy Environ. Sci.* **2012**, *5*, 7526–7530. [CrossRef]

14. Wang, J.Y.; Mei, X.Y.; Huang, L.; Zheng, Q.W.; Qiao, Y.Q.; Zang, K.T.; Mao, S.C.; Yang, R.Y.; Zhang, Z.; Gao, Y.S.; Guo, Z.H.; Huang, Z.G.; et al. Synthesis of layered double hydroxides/graphene oxide nanocomposite as a novel high-temperature CO_2 adsorbent. *J. Energy Chem.* **2015**, *24*, 127–137. [CrossRef]

15. Gao, Y.; Zhang, Z.; Wu, J.; Yi, X.; Zheng, A.; Umar, A.; O'Hare, D.; Wang, Q. Comprehensive investigation of CO_2 adsorption on Mg–Al–CO_3 LDH-derived mixed metal oxides. *J. Mater. Chem. A* **2013**, *1*, 12782. [CrossRef]

16. Qiao, Y.; Wang, J.; Zhang, Y.; Gao, W.; Harada, T.; Huang, L.; Hatton, T.A.; Wang, Q. Alkali Nitrates Molten Salt Modified Commercial MgO for Intermediate-Temperature CO_2 Capture: Optimization of the Li/Na/K Ratio. *Ind. Eng. Chem. Res.* **2017**, *56*, 1509–1517. [CrossRef]

17. Al-Jeboori, M.J.; Fennell, P.S.; Nguyen, M.; Peng, K. Effects of Different Dopants and Doping Procedures on the Reactivity of CaO-based Sorbents for CO_2 Capture. *Energy Fuels* **2012**, *26*, 6584–6594.

18. Chen, S.Y.; Xiang, W.G.; Wang, D.; Xue, Z.P. Incorporating IGCC and CaO sorption-enhanced process for power generation with CO_2 capture. *Appl. Energy* **2012**, *95*, 285–294. [CrossRef]

19. Pfeiffer, H.; Lima, E.; Bosch, P. Lithium-Sodium Metazirconate Solid Solutions, $Li_{2-x}Na_xZrO_3$ (0 <= x <= 2): A Hierarchical Architecture. *Chem. Mater.* **2006**, *18*, 2642–2647. [CrossRef]

20. Zheng, Q.W.; Huang, L.; Zhang, Y.; Wang, J.Y.; Zhao, C.Z.; Zhang, Q.; Zheng, W.J.; Cao, D.P.; O'Hared, D.; Wang, Q. Unexpected highly reversible topotactic CO_2 sorption/desorption capacity for potassium dititanate. *J. Mater. Chem. A* **2016**, *4*, 12889–12896. [CrossRef]

21. Rodríguez, M.T.; Pfeiffer, H. Sodium metasilicate (Na_2SiO_3): A thermo-kinetic analysis of its CO_2 chemical sorption. *Thermochim. Acta* **2008**, *473*, 92–95. [CrossRef]

22. Romero-Ibarra, I.C.; Ortiz-Landeros, J.; Pfeiffer, H. Microstructural and CO_2 chemisorption analyses of Li_4SiO_4: Effect of surface modification by the ball milling process. *Thermochim. Acta* **2013**, *567*, 118–124. [CrossRef]

23. Reddy, M.K.R.; Xu, Z.P.; Lu, G.Q.; da Costa, J.C.D. Influence of water on high-temperature CO_2 capture using layered double hydroxide derivatives. *Ind. Eng. Chem. Res.* **2008**, *47*, 2630–2635. [CrossRef]

24. Qiao, Y.Q.; Wang, J.Y.; Huang, L.; Zheng, Q.W.; O'Hare, D.; Wang, Q. LDH/$MgCO_3$ hybrid multilayer on an aluminium substrate as a novel high-temperature CO_2 adsorbent. *RSC Adv.* **2015**, *5*, 82777–82780. [CrossRef]

25. Qin, Q.; Wang, J.; Zhou, T.; Zheng, Q.; Huang, L.; Zhang, Y.; Lu, P.; Umar, A.; Louis, B.; Wang, Q. Impact of organic interlayer anions on the CO_2 adsorption performance of Mg-Al layered double hydroxides derived mixed oxides. *J. Energy Chem.* **2017**. [CrossRef]

26. Sanna, A.; Ramli, I.; Maroto-Valer, M.M. Development of sodium/lithium/fly ash sorbents for high temperature post-combustion CO_2 capture. *Appl. Energy* **2015**, *156*, 197–206. [CrossRef]

27. Wang, K.; Guo, X.; Zhao, P.; Wang, F.; Zheng, C. High temperature capture of CO_2 on lithium-based sorbents from rice husk ash. *J. Hazard. Mater.* **2011**, *189*, 301–307. [CrossRef] [PubMed]

28. Niu, M.Y.; Li, X.Y.; Ouyang, J.; Yang, H.M. Lithium orthosilicate with halloysite as silicon source for high temperature CO_2 capture. *RSC Adv.* **2016**, *6*, 44106–44112. [CrossRef]

29. Nguyen, A.N.; Reinert, L.; Leveque, J.M.; Beziat, A.; Dehaudt, P.; Juliaa, J.F.; Duclaux, L. Preparation and characterization of micron and submicron-sized vermiculite powders by ultrasonic irradiation. *Appl. Clay Sci.* **2013**, *72*, 9–17. [CrossRef]

30. Duman, O.; Tunc, S.; Polat, T.G. Determination of adsorptive properties of expanded vermiculite for the removal of C.I. Basic Red 9 from aqueous solution: Kinetic, isotherm and thermodynamic studies. *Appl. Clay Sci.* **2015**, *109*, 22–32. [CrossRef]

31. Stawinski, W.; Freitas, O.; Chmielarz, L.; Wegrzyn, A.; Komedera, K.; Blachowski, A.; Figueiredo, S. The influence of acid treatments over vermiculite based material as adsorbent for cationic textile dyestuffs. *Chemosphere* **2016**, *153*, 115–129. [CrossRef] [PubMed]

32. Adpakpang, K.; Patil, S.B.; Oh, S.M.; Kang, J.H.; Lacroix, M.; Hwang, S.J. Effective Chemical Route to 2D Nanostructured Silicon Electrode Material: Phase Transition from Exfoliated Clay Nanosheet to Porous Si Nanoplate. *Electrochim. Acta* **2016**, *204*, 60–68. [CrossRef]

33. Ryu, J.; Hong, D.; Choi, S.; Park, S. Synthesis of Ultrathin Si Nanosheets from Natural Clays for Lithium-Ion Battery Anodes. *ACS Nano* **2016**, *10*, 2843–2851. [CrossRef] [PubMed]

34. Ryu, J.; Jang, Y.J.; Choi, S.; Kang, H.J.; Park, H.; Lee, J.S.; Park, S. All-in-one synthesis of mesoporous silicon nanosheets from natural clay and their applicability to hydrogen evolution. *NPG Asia Mater.* **2016**, *8*, e248. [CrossRef]

35. Olivares-Marín, M.; Drage, T.C.; Maroto-Valer, M.M. Novel lithium-based sorbents from fly ashes for CO_2 capture at high temperatures. *Int. J. Greenh. Gas Control* **2010**, *4*, 623–629. [CrossRef]

36. Wang, K.; Zhao, P.; Guo, X.; Li, Y.; Han, D.; Chao, Y. Enhancement of reactivity in Li_4SiO_4-based sorbents from the nano-sized rice husk ash for high-temperature CO_2 capture. *Energy Convers. Manag.* **2014**, *81*, 447–454. [CrossRef]

37. Li, R.G.; Zhu, J.Q.; Zhou, W.B.; Cheng, X.M.; Li, Y.Y. Thermal properties of sodium nitrate-expanded vermiculite form-stable composite phase change materials. *Mater. Des.* **2016**, *104*, 190–196. [CrossRef]

38. Tian, W.L.; Kong, X.G.; Jiang, M.H.; Lei, X.D.; Duan, X. Hierarchical layered double hydroxide epitaxially grown on vermiculite for Cr(VI) removal. *Mater. Lett.* **2016**, *175*, 110–113. [CrossRef]

39. Perez-Maqueda, L.A.; Maqueda, C.; Perez-Rodriguez, J.L.; Subrt, J.; Cerny, Z.; Balek, V. Thermal behaviour of ground and unground acid leached vermiculite. *J. Therm. Anal. Calorim.* **2011**, *107*, 431–438. [CrossRef]

40. El Mouzdahir, Y.; Elmchaouri, A.; Mahboub, R.; Gil, A.; Korili, S.A. Synthesis of nano-layered vermiculite of low density by thermal treatment. *Powder Technol.* **2009**, *189*, 2–5. [CrossRef]

41. Wang, Q.; Wu, Z.; Tay, H.H.; Chen, L.; Liu, Y.; Chang, J.; Zhong, Z.; Luo, J.; Borgna, A. High temperature adsorption of CO_2 on Mg–Al hydrotalcite: Effect of the charge compensating anions and the synthesis pH. *Catal. Today* **2011**, *164*, 198–203. [CrossRef]

42. Wang, Q.; Tay, H.H.; Ng, D.J.; Chen, L.; Liu, Y.; Chang, J.; Zhong, Z.; Luo, J.; Borgna, A. The effect of trivalent cations on the performance of $Mg-M-CO_3$ layered double hydroxides for high-temperature CO_2 capture. *ChemSusChem* **2010**, *3*, 965–973. [CrossRef] [PubMed]

43. Wang, Q.; Tay, H.H.; Chen, L.; Liu, Y.; Chang, J.; Zhong, Z.; Luo, J.; Borgna, A. Preparation and CO_2 Capture Capacity of Alkali Metal Carbonates Promoted Hydrotalcite. *J. Nanoeng. Nanomanuf.* **2011**, *1*, 298–303. [CrossRef]

44. Wang, Q.; Gao, Y.; Luo, J.; Zhong, Z.; Borgna, A.; Guo, Z.; O'Hare, D. Synthesis of nano-sized spherical $Mg_3Al–CO_3$ layered double hydroxide as a high-temperature CO_2 adsorbent. *RSC Adv.* **2013**, *3*, 3414. [CrossRef]

45. Wang, Q.; Tay, H.H.; Guo, Z.; Chen, L.; Liu, Y.; Chang, J.; Zhong, Z.; Luo, J.; Borgna, A. Morphology and composition controllable synthesis of $Mg–Al–CO_3$ hydrotalcites by tuning the synthesis pH and the CO_2 capture capacity. *Appl. Clay Sci.* **2012**, *55*, 18–26. [CrossRef]

46. Duan, Y.; Pfeiffer, H.; Li, B.; Romero-Ibarra, I.C.; Sorescu, D.C.; Luebke, D.R.; Halley, J.W. CO_2 capture properties of lithium silicates with different ratios of Li_2O/SiO_2: An ab initio thermodynamic and experimental approach. *Phys. Chem. Chem. Phys.* **2013**, *15*, 13538–13558. [CrossRef] [PubMed]